A Study on the Rheological Properties and Processability of Polycarbonate

Young-Cheol Ahn, Hyo-Jun Kim

Division of Chemical Engineering, Kyungnam University, Masan 631-701, Korea

Received 21 February 2002; accepted 24 May 2002

ABSTRACT: The transport theory for the solids conveying zone in a single-screw extruder was applied to calculate the pressure distributions along the screw channel for several bisphenol A polycarbonate resins based on the screw revolution speed and the flow rate. The pressure distributions and the flow rates of the resins were related to the structural and rheological properties. When polymers have the same chemical structure and number-average molecular weight and the same mechanical properties, the polymer having a broader molecular weight distribution showed a lower glass transition temperature. For the polymer with broader MWD a relatively low pressure was developed along the screw channel, and an increased flow rate was observed. A relatively short melting length was also observed for this polymer and, accordingly, it was concluded that the polymer with a broader MWD has a better processability. © 2002 Wiley Periodicals, Inc. J Appl Polym Sci 86: 2921–2929, 2002

Key words: structure; property; molecular weight distribution; polycarbonates

INTRODUCTION

Einhorn first synthesized polycarbonate in the late 1890s from phosgene, resorcinol, and hydroquinone, which is an amorphous material showing thermoplastic property.[1,2] The polymer has a carbonate bond in its main chain and the bisphenol A type occupies most of the polymer group. From the structural point of view the polymer contains aromatic component that makes it less flexible, noncrystalline, hard, and thermally stable, whereas it has a high glass transition temperature that makes it hard to process. Especially in processing a sheet product a highly viscous and high molecular weight polymer is used, which makes the processing harder, and inevitably urges to adopt an extrusion process.

Extrusion is one of the most important processes in polymer processing. It is to produce such items as sheets, films, pipes, etc., from the solid pellets or powders of polymers that are sent into the barrel, and then melted and passed through dies of arbitrary shape. An extruder consists of the three parts, which are the solids conveying zone, the melting zone, and the metering zone. Each part should be studied via different ways of approach to understand the peculiar phenomena occurring in each zone. For the solids conveying zone, Darnell and Mol[3] studied systematically the single-screw extruder in 1956, and Tadmor and Klein[4] expanded the theory further in 1970. Tadmor and Broyer[5,6] considered the anisotropic pressure acting on the solids bed and proposed a nonisothermal model. Tadmor and Kacir[7] insisted that a delay zone is formed at the end of the solids conveying zone just before the start of the steady-state melting mechanism. In 1974, Lovegrove and Williams[8] expanded the concept of initial pressure considering the volumetric force that had been ignored before. In 1991, Zhu et al.[9] proposed a nonplug flow-type theory by treating the inner friction as a parameter. In 1992, Campbell et al.[10] reported the importance of a screw helix in conveying solids, and in 1995, Campbell and Dontula[11] suggested new models assuming the additional normal force acting on the solids bed is the same as the frictional force between the barrel and the solids bed.

To understand the extrusion process correctly, data for the solids conveying, melting, flow, and stress distributions are needed together with the rheological phenomena in downstream processes including an extrudate swell. These are directly related to the physical properties of polymers, and therefore, the properties and characteristics of a polymer should be measured and recognized. In this study, the structure and properties of polycarbonates were analyzed, and the pressure development along the screw channel was calculated using the screw revolution speed and flow rate that were experimentally obtained, based on the theories of solids conveying. They were compared with each other to identify the extrusion processing characteristics of polycarbonate.

THEORETICAL MODEL

Analysis of the solids conveying is generally based on the model developed by Tadmor and Klein[4] from the theory of Darnell and Mol.[3] In this study the following assumptions were made to obtain the pressure equa-

Correspondence to: Y.-C. Ahn (ycahn@kyungnam.ac.kr).

Contract grant sponsor: Kyungnam University Research Fund, 2001.

Journal of Applied Polymer Science, Vol. 86, 2921–2929 (2002)
© 2002 Wiley Periodicals, Inc.

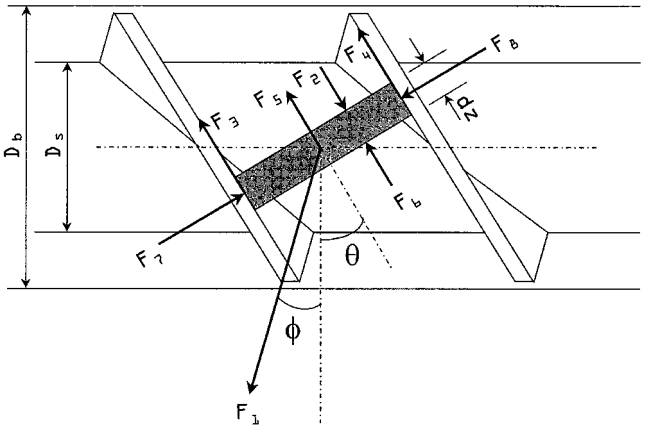

Figure 1 Schematic diagram of the forces acting on the differential solids bed in the screw channel.

tion along the channel in terms of the screw revolution speed: (1) channel depth is uniform; (2) gravitational force is negligible; (3) frictional coefficient is irrespective of the pressure; (4) solid particles form a continuous phase; (5) barrel is rotating instead of the screw; (6) variation of density in the solids bed is negligible; (7) solids bed moves in a plug-flow pattern; and (8) solids bed contacts with the wall of screw channel.

Figure 1 shows eight forces acting on the differential bed in the solids conveying zone. F_1 is the frictional force between the solids bed and the barrel, F_2 is the force acting on the solids bed by the pressure p, F_3 is the frictional force between the solids bed and the rear screw flight, F_4 is the frictional force between the solids bed and the fore screw flight, F_5 is the frictional force between the solids bed and the screw surface, F_6 is the force acting on the solids bed by the pressure $p + dp$, F_7 is the normal force acting on the solids bed by the rear screw flight, and F_8 is the normal force acting on the solids bed by the fore screw flight. If the frictional coefficient of the barrel is f_b, that of the screw is f_s, the distance in the downstream channel is z, the channel width is W, and the channel depth is H, then these eight forces can be expressed as in Table I, where dz is the differential thickness of the solids bed and dp is the pressure difference over dz. The additional normal force F^* in F_7 remains unknown, but it can be calculated from the known variables by setting the total axial force and the total torque equal to zero.

The pressure variation along the channel can be obtained by integrating the force balance equations for the differential domain of interest and is described as follows.

$$p = p_0 \exp\left[\frac{(-A_1K + B_1)z}{A_2K + B_2}\right] \tag{1}$$

where

$$A_1 = f_bW \sin\phi + f_sW \sin\theta + 2f_sH \sin\theta$$

$$A_2 = HW \sin\theta$$

$$B_1 = f_bW \cos\phi - 2f_sH \cos\theta \frac{\bar{D}}{D_b} - f_sW \cos\theta \frac{D_s}{D_b}$$

$$B_2 = HW \cos\theta \frac{\bar{D}}{D_b}$$

$$K = \frac{\bar{D}}{D_b} \frac{\sin\theta + f_s \cos\theta}{\cos\theta - f_s \sin\theta}$$

$$\bar{D} = \frac{D_b + D_s}{2}$$

and D_b and D_s are the diameters of the barrel and the screw, respectively, as shown in Figure 1. In eq. (1) p_o is the pressure at the entrance ($z = 0$) that is obtained statically from the height of the packed bed and ϕ is the angle that the relative velocity of the barrel to the solids bed will make with the tangent direction and is a function of the flow rate and the structure and can be obtained from the flow rate. θ is the angle that the screw flight will make with the direction tangent.

The flow rate Q_s can be obtained by multiplying the axial velocity of the solids bed with the cross-sectional area of the channel and is described as eq. (2).

$$Q_s = V_b\left(\frac{\tan\theta \tan\phi}{\tan\theta + \tan\phi}\right)\left[\frac{\pi}{4}(D_b^2 - D_s^2) - \frac{eH}{\sin\theta}\right] \tag{2}$$

where V_b is the linear velocity of the barrel, and e is the thickness of the screw flight. When the screw revolution speed is N rpm, the linear velocity of the barrel V_b

TABLE I
Expressions of the Forces Acting on the Differential Solids Bed

F_1	Frictional force between the solids bed and the barrel	$f_b\,pW\,dz$
F_2	Force acting on the solids bed by pressure p	$HW\,p$
F_3	Friction force between the solids bed and the rear flight	F_7f_s
F_4	Friction force between the solids bed and the fore flight	F_8f_s
F_5	Friction force between the solids bed and the screw surface	$f_spW\,dz$
F_6	Force acting on the solids bed by pressure $p + dp$	$HW\,(p + dp)$
F_7	Normal force acting on the solids bed by the rear flight	$pHdz + F^*$
F_8	Normal force acting on the solids bed by the fore flight	$pHdz$

TABLE II
Dimensions of the Extruder

Barrel diameter	D_b	0.0497 m
Screw diameter	D_s	0.0349 m
Flight thickness	e	0.00745m
Channel width	W	0.0435 m
Channel depth	H	0.0074 m (Feeding zone)
Flight angle	θ	15°

is $\pi D_b N$. Equation (2) can be rearranged with respect to the angle ϕ as follows:

$$\tan\phi = \frac{C\tan\theta}{1-C} \tag{3}$$

where

$$C = \frac{1}{\tan\theta}\frac{Q_s}{V_b}\frac{1}{\left[\frac{\pi}{4}(D_b^2 - D_s^2) - \frac{eH}{\sin\theta}\right]}.$$

The melting length where the solids completely melt can be derived from the balance equation for the melt film as follows:

$$L_{\text{melting}|X=0} = \frac{2\rho_s V_{sz} H W^{0.5}}{\Phi} \tag{4}$$

$$\Phi = \left\{\frac{V_{bx}\rho\left[k_m(T_b - T_m) + \frac{\mu}{2}V_j^2\right]}{2[C_{ps}(T_m - T_s) + \lambda]}\right\}^{1/2} \tag{5}$$

where X is the width of the solids bed, V_{bx} the normal component of the velocity of the barrel to the screw flight, V_j the relative velocity of the barrel to the solids bed, ρ the density of the melt, ρ_s the density of the solids, k_m the thermal conductivity of the melt, C_{ps} the heat capacity of the solids, μ the viscosity of the melts, λ the latent heat of the solids, T_m the melting point of the resin, and T_b and T_s the temperatures of the barrel and the screw, respectively.

EXPERIMENTAL

Sample materials

The resins used for analysis were polycarbonates that were commercially available and had grades of low to medium viscosities. They were all bisphenol A polycarbonates and named PC-A, PC-B, and PC-C.

Infrared spectrometry

Chemical structures of the sample materials were analyzed using Fourier transform infrared spectrometer (Mattson Inc., Research I series). The samples were cast into films by the solution casting method in which methylene chloride was used as the solvent. The solutions were cast on glass plates and dried at 120°C for 5 h in a vacuum drying oven.

Nuclear magnetic resonance spectrometry

End-group patterns of the samples were observed using Fourier transform nuclear magnetic resonance spectrometer (Varian Inc., Unity Inova 400 *M*Hz) for ^{1}H and ^{13}C with d-chloroform as the solvent.

Gel permeation chromatography

Molecular weight and its distribution were measured with gel permeation chromatography (Waters Inc., 150CV-ALC/GPC). The columns were μ-styragel series (pore size 10^5, 10^4, 10^3, 500 Å), and the solvent was tetrahydrofuran with flow rate of 2 mL/min. Polycarbonate was used for the standard, and refractive index (Waters Inc., R410) was used for detection.

Mechanical properties

Impact strength and ultimate tensile strength were measured with Izod impact tester (Toyoseiki Inc., DG-IB) and universal tensile system (Lloyd Instruments Inc., LR30K), respectively. The impact test samples were injection molded to have dimensions of 64 × 12.8 × 3.2 mm, and had notches of 2.54 mm to concentrate the stress. The tensile test samples were also injection molded with type M-I described in ASTM D638, and tested at room temperature with a crosshead speed of 50 mm/min. A total of seven samples were tested for each grade, and five of them, excluding the highest and lowest values, were averaged.

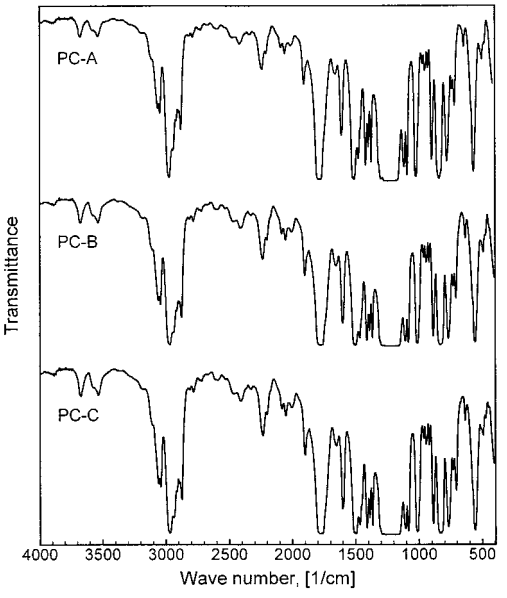

Figure 2 FTIR spectra of the three polycarbonate resins.

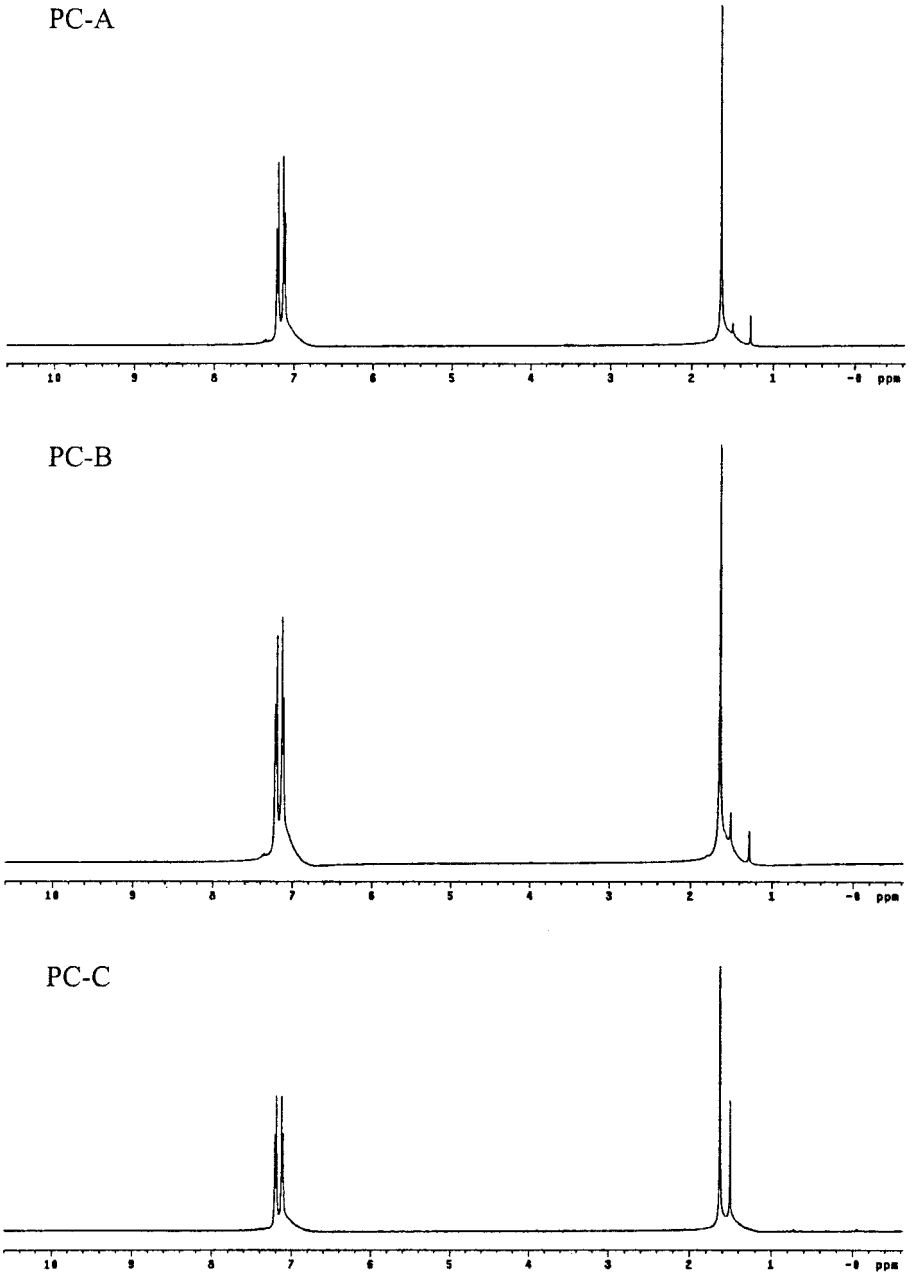

Figure 3 ^{1}H FT-NMR spectra of the three polycarbonate resins.

Differential scanning calorimetry

Glass transition temperature and melting point were measured using a differential scanning calorimeter (TA Instruments Inc., DSC-10). The DSC was calibrated with indium (T_m = 156.60°C) and zinc (T_m = 419.58°C). The samples were thermally scanned twice such that first they were heated up from 50 to 280°C to measure the glass transition temperature and melting point, then were cooled down to the room temperature. and second, heated up again from 50 to 280°C to measure the glass transition temperature. Nitrogen gas was used as inert gas with the flow rate of 20 mL/min. The melting point was determined by the onset point, while the glass transition temperature was determined by the onset and inflection point of the second scan. The glass transition temperature of the first scan was discarded, considering a possible existence of the thermal hysterisis caused by the manufacturing process.

Rheological property measurement

Shear viscosity was measured using the twin bore capillary rheometer (Rosand Inc., Advanced Rheometer System) while viscoelasticity was measured using the rheometrical dynamic spectrometer (Rheometrics, RDS-II). The dies used in the capillary rheometer had dimensions of 32 × 1, 32 × 2, 16 × 1, 16 × 2, and 8

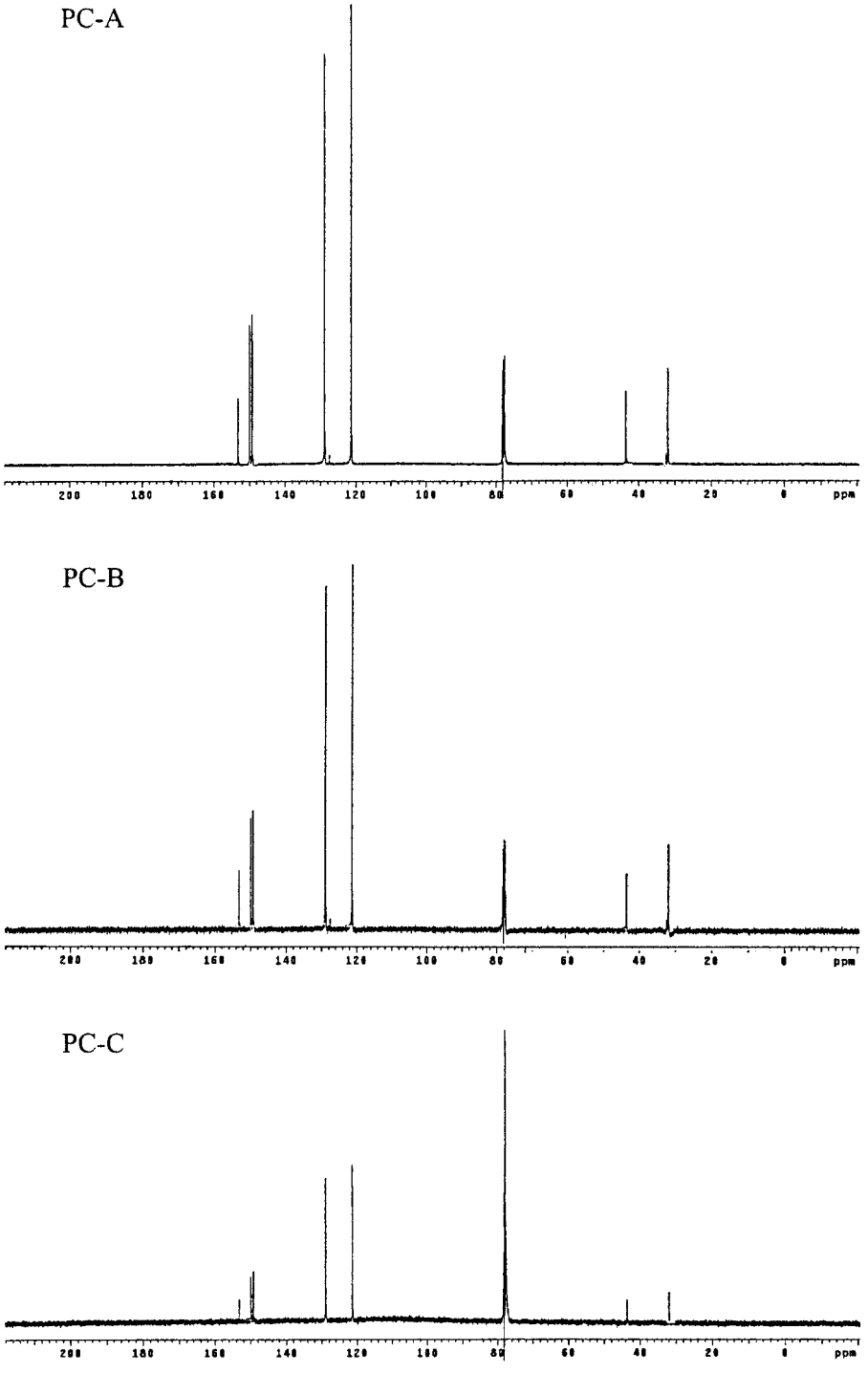

Figure 4 ^{13}C FT-NMR spectra of the three polycarbonate resins.

$\times$ 0.5 (L $\times$ D). The range of shear rate was 100–5000 s^{-1}, and the measuring temperatures were 280, 300, and 320°C. In rheometrical dynamic spectrometry the cone-and-plate fixture had a radius of 12.5 mm and an angle of 0.04 rad. The angular velocity was changed from 0.2 to 500 rad/s, with temperatures of 260, 280, and 300°C to measure the storage modulus, loss modulus, and dynamic viscosity.

Extrusion experiment

The flow rate of polycarbonate was measured in terms of the screw revolution speed using a single-screw extruder with a barrel diameter of 50 mm. The barrel temperature was set at 290°C and the resin was dried at 120°C for 4 h in a vacuum drying oven. The resin was supplied into a hopper that was equipped with a

TABLE III
Average Molecular Weights and Polydispersity Indices of the Polycarbonate Resins

Sample	M_n	M_w	M_z	Polydispersity Index
PC-A	9800	24,900	39,300	2.54
PC-B	10,900	30,000	50,300	2.75
PC-C	10,700	31,100	51,100	2.91

hot air drying oven operating at 120°C. The screw revolution speeds of 10, 15, 20, and 25 rpm were chosen, and the flow rates of the resin were measured. The major dimensions of the extruder were shown in Table II.

RESULTS AND DISCUSSION

Chemical structure

According to the Fourier transform infrared spectrums shown in Figure 2, there are no difference between the three samples. The Fourier transform nuclear magnetic resonance spectrums of these samples also showed the same peaks in ^1H and ^{13}C resonance, as can be seen in Figures 3–4. Therefore, it can be said that these samples have the same chemical structures.

Molecular weight and its distribution

For the three resins the molecular weight and its distribution were measured using gel permeation chromatography and summarized in Table III. The sample PC-C has a number-average molecular weight of 10,700, which is close to that of PC-B, while it has a polydispersity index of 2.91, which is the largest among the three. From this it can be said that the sample PC-C's weight-average molecular weight is higher than PC-B's, which means that the PC-C has more of the extremely large molecules. This can be confirmed from the *z*-average molecular weight. The polydispersity, M_w/M_n, of PC-B is 2.75 and that of PC-C is 2.91. The difference of 0.16 is not small in such a condensate polymer as polycarbonate for which the polydispersity does not vary so much as for the radically polymerized polymer. Dealy and Wissbrun[12] insisted that although the equations relating compliance to MWD, expressed in terms of $(M_z/M_w)^a$ or M_zM_{z+1}/M_w^2, are to reflect the contributions of the high molecular weight components, it is the most difficult to detect the high molecular weight components precisely. However, especially for the log normal MWD, those equations reduce to a proportional function of $(M_w/M_n)^3$. In this case, M_w/M_n of 2.75 corresponds to $(M_w/M_n)^3$ of 20.8, while M_w/M_n of 2.91 corresponds to $(M_w/M_n)^3$ of 24.6, which means 18% difference in compliance. Van Krevelen[13] also thought that expressing the MWD in terms of M_w/M_n is more desirable.

TABLE IV
Ultimate Tensile Strength and Impact Strength of the Polycarbonate Resins

	PC-A	PC-B	PC-C
Ultimate tensile strength (MPa)	67.55 ± 1.48	68.87 ± 0.81	69.05 ± 0.64
Impact strength (kJ/m^2)	7.33 ± 0.15	8.03 ± 0.15	8.24 ± 0.14

TABLE V
Glass Transition Temperatures and Melting Points of the Polycarbonate Resins

Sample	$T_{g'onset}$ [°C]	$T_{g'inf}$ [°C]	T_m [°C]
PC-A	149.68	154.26	215.23 (Observed at the 1st scan only)
PC-B	153.36	157.11	Not observed
PC-C	146.93	152.03	Not observed

Mechanical properties

The ultimate tensile strength and the Izod impact strength of the samples were measured and summarized in Table IV. The sample PC-A that had the lowest number-average molecular weight showed the relatively low ultimate tensile strength and Izod impact strength, while the samples PC-B and PC-C, which have a little bit larger number-average molecular weights that were almost the same, showed similar ultimate tensile strength and Izod impact strength.

Thermal characteristics

The results of thermal analysis for the samples using DSC were summarized in Table V. The glass transition temperature generally increases with molecular weight as in PC-A and PC-B, while the glass transition temperature of PC-C was 146.93°C, that is very low compared to those of PC-A and PC-B, which have lower or equivalent molecular weight to PC-C. This difference can be explained to come from the molecular weight distribution, that is, because the polydispersity of PC-C is larger than that of PC-B even though the number-average molecular weights of both resins are equal, PC-C becomes more flexible than that of PC-B. From this result, it can be said that the resin PC-C is easier to be processed than the others. It is interesting to see that in the first scan of PC-A there appeared a melting peak that was not expected to be observed for such an amorphous polymer as polycarbonate, but in the second scan it disappeared. The hysterisis in manufacturing process is considered to be the cause of this phenomenon.

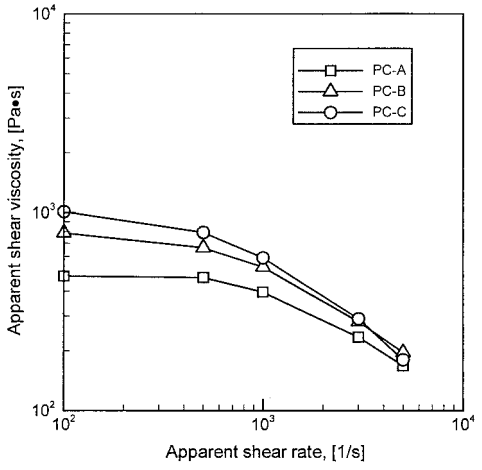

Figure 5 Shear viscosities of the polycarbonate resins measured with capillary rheometer at 300°C.

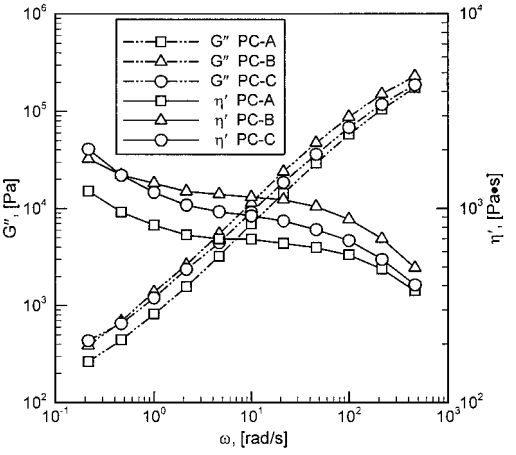

Figure 7 Loss moduli and in-phase viscosities of polycarbonate resins measured with RDS at 280°C.

Rheological properties

The shear viscosity measured at 300°C was shown in Figure 5. As the shear rate is increased, the viscosity is monotonically decreased. When the shear rate is 100 s^{-1}, the shear viscosity is 500–1000 Pa · s, while when the shear rate is 5000 s^{-1}, the shear viscosity is 150–200 Pa · s.

The viscoelastic properties were measured at 260, 280, and 300°C using a rheometric dynamic spectrometer. The storage modulus G', the loss modulus G'', the in- and out-of-phase viscosities η' and η'' were obtained in the frequency range of 0.2–500 rad/s. The viscoelastic properties measured at 280°C were shown in Figures 6–7. As the frequency was increased, the moduli increased monotonically while the dynamic viscosities decreased monotonically. It is interesting to see in Figure 6 that both the storage modulus G' and the out-of-phase viscosity η'' of the resins PC-B and PC-C are overturned as the frequency is increased above 15 rad/s. That is, in the frequency range below 15 rad/s the storage modulus and the out-of-place viscosity of PC-C are larger than those of PC-B, while in the frequency range above 15 rad/s they become smaller than those of PC-B. Similar phenomena were observed for the loss modulus G'' and the in-phase viscosity η' as shown in Figure 7, where the loss modulus and the in-phase viscosity of PC-C are larger than those of PC-B in the frequency range below 0.4 rad/s, and they become smaller in the frequency range above 0.4 rad/s. These phenomena are attributed to the relatively broad distribution of molecular weight of PC-C compared to that of PC-B, as we have previously discussed about concerning the compliance in the molecular weight and its distribution section. In relation to the molecular weight distribution, it can be thought that the polymer having broad molecular weight distribution has a relatively large number of both low and high molecular weight components compared to the narrow MWD one. It is the high molecular weight component that makes the storage modulus increased at the low frequency, while it is the low molecular weight component that makes the loss modulus increased at the high frequency. When the shear rate is increased in a tube flow, the high molecular weight component moves into the core section while the low molecular weight component moves to the wall side. It is this low molecular weight component at the wall side that reduce the shear stress dramatically, and, thus, this may be compared to the phenomenon that the highly viscous polymer moves into the core while the low molecular weight polymer moves outward to the wall.[14] This can be interpreted as that the PC-C, compared to PC-B is less sagging at low shear rate because of the high modulus and dynamic viscosity, while it shows low stress at high shear rate because of the low modulus and dynamic viscosity. Similar phenomena were observed at the temperatures of 260 and 300°C. Therefore, it can be said that the PC-C has a better processability compared to PC-B and, because the only difference be-

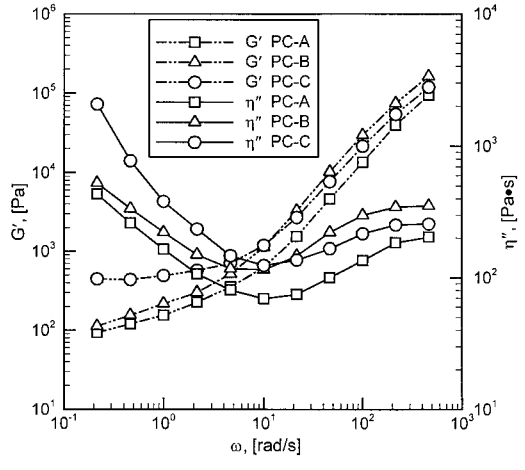

Figure 6 Storage moduli and out-of-phase viscosities of polycarbonate resins measured with RDS at 280°C.

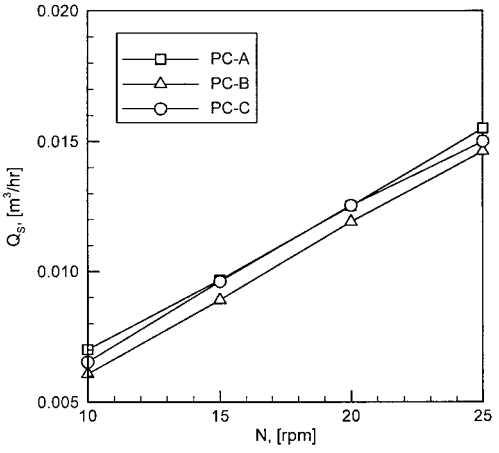

Figure 8 Volumetric flow rates of the polycarbonate resins expressed as a function of the screw revolution speed.

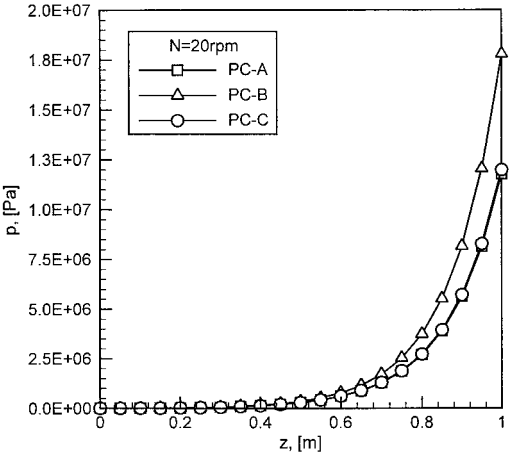

Figure 10 Pressure distributions along the downstream distance of the channel calculated at the screw revolution speed of 20 rpm.

tween them is the molecular weight distribution, it also can be said that the polycarbonate with broader molecular weight distribution has a better processability.

Transport properties in extruder

As we have seen above the polycarbonates PC-C and PC-B have the same mechanical properties, chemical structures, and molecular weights but different molecular weight distributions, which results in different processability. The difference in processability was tested through an extrusion experiment. In the theories developed previously the angle ϕ can be calculated once the flow rate Q_s is determined and, by applying Q_s and ϕ into eq. (1) the pressure variation along the downstream distance of the channel can be obtained as a function of screw revolution speed. In Figures 8–9, the variations of Q_s and ϕ are shown as functions of the screw revolution speed of the single screw extruder. We can see that at each screw revolution speed the polycarbonate PC-C has higher flow rate than PC-B and almost the same flow rate compared even to the lower molecular weight polycarbonate PC-A. The size of angle ϕ is determined according to how fast the solid resin moves and this is directly related to the frictional coefficient. According to Figure 9, the frictional coefficients of PC-A and PC-C are thought to be relatively large compared to that of PC-B. It is generally accepted that the polymers with low molecular weight and/or broad molecular weight distribution have relatively large frictional coefficient. Also, in view of the thermal characteristics the polymer with low molecular weight and/or broad molecular weight distribution will have a low glass transition temperature so that it may reach the rubbery state more easily, which leads to high frictional coefficient. Because the frictional coefficient is a function of temperature and pressure, it must be studied more systematically in the future.

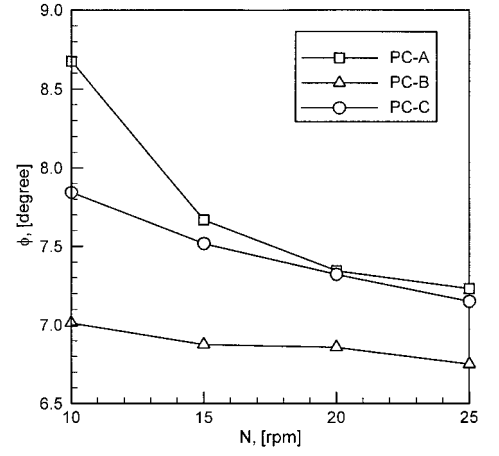

Figure 9 Angles that the relative velocity of the barrel to the solids bed makes with the tangent direction, expressed as a function of the screw revolution speed.

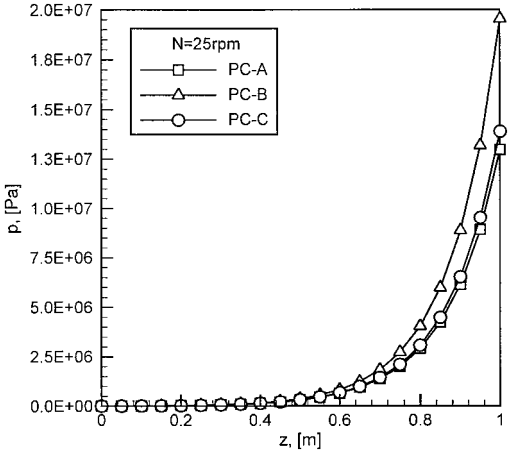

Figure 11 Pressure distributions along the downstream distance of the channel calculated at the screw revolution speed of 25 rpm.

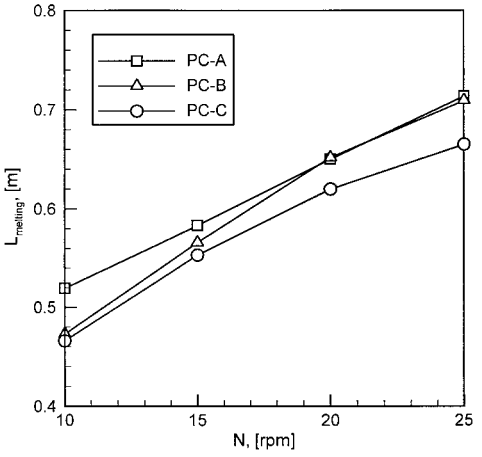

Figure 12 Melting lengths of the polycarbonate resins expressed as a function of the screw revolution speed.

For the screw revolution speed of 20 and 25 rpm, the variations of pressure along the downstream distance of the channel were obtained and are displayed in Figures 10–11. Here we can see that the pressure developed by PC-C is lower than the pressure by PC-B, and is almost the same as the pressure by PC-A.

In Figure 12, the melting lengths of these polycarbonate grades are shown as a function of the screw revolution speed. The melting length was defined as the downstream distance of the channel where all the solids melt down to liquid, i.e., $X = 0$. For the screw revolution speeds tested the melting length of PC-C was the shortest, especially for the screw revolution speed over 20 rpm, where PC-B had the same melting length as PC-A.

Based on the results discussed above, it can be said that among the polycarbonate resins that have the same mechanical properties, chemical structure, and number-average molecular weight as others the one with a broader molecular weight distribution has a better processability than the others. This corresponds to the previous results obtained for the rheologic properties.

CONCLUSIONS

The chemical structure and physical properties of the bisphenol A polycarbonates were measured and their transport phenomena in solids conveying zone of a single-screw extruder were studied theoretically and experimentally. The processability of those polycarbonates that is a function of the chemical structure and physical properties of the polymer was identified in an extrusion process by investigating the variations of pressure along the downstream distance of the channel at various screw revolution speeds. For the polycarbonate resins tested it was found that when the polymers have the same mechanical properties, chemical structures, and number-average molecular weights, the one having broader molecular weight distribution would be softened more easily because of the lower glass transition temperature, would have a better drapery property at low shear rate, would develop lower stress at high shear rate because of the low modulus and dynamic viscosity, would have a higher flow rate while lower pressure distribution in solids bed, and thus, would be said to have a better processability.

This work was supported by the Kyungnam University Research Fund, 2001.

References

1. Einhorn, H. Jestus Liebigs Ann Chem 1898, 300, 135.
2. Schnell, H. Chemistry and Physics of Polycarbonates; Interscience: New York, 1964.
3. Darnell, W. H.; Mol, E. A. J. SPE J 1956, 12, 20.
4. Tadmor, Z.; Klein, I. Engineering Principles of Plasticating Extrusion; Van Nostrand Reinhold: New York, 1970.
5. Tadmor, Z.; Broyer, E. Polym Eng Sci 1972, 12, 12.
6. Tadmor, Z.; Broyer, E. Polym Eng Sci 1972, 12, 378.
7. Tadmor, Z.; Kacir, L. Polym Eng Sci 1972, 12, 387.
8. Lovegrove, J. G. A.; Williams, J. G. Polym Eng Sci 1974, 14, 589.
9. Zhu, F.; Chen, L.; Fang, S. Polym Eng Sci 1991, 31, 1117.
10. Campbell, G. A.; Sweeney, P. A.; Felton, J. N. Polym Eng Sci 1992, 32, 1765.
11. Campbell, G. A.; Dontula, N. Int Polym Process X 1995, 1, 30.
12. Dealy, J. M.; Wissbrun, K. F. Melt Rheology and Its Role in Plastics Processing; Van Nostrand Reinhold: New York, 1990.
13. Van Krevelen, D. W. Properties of Polymers; Elesevier: Amsterdam, 1997, 3rd ed.
14. Han, C. D. Rheology in Polymer Processing; Academic Press: New York, 1976, Chap 10.